J. Comput. Appl. Res. Mech. Eng. Vol. 13. No. 1, pp. 27-38, 2023 *DOI: 10.22061/JCARME.2023.9255.2239*

SRTTU

Journal of Computational and Applied Research in Mechanical Engineering

jcarme.sru.ac.ir

JCARME

ISSN: 2228-7922

Research paper

Predictive model for diameter control of polysulfone hollow fibers produced by dry-jet wet spinning

A. Rugbani*

Department of Mechanical and Mechatronic Engineering, Cape Peninsula University of Technology, Cape Town, South Africa

Article info:

Article history:

Received: 27/08/2022

Revised: 05/07/2023

Accepted: 07/07/2023

Online: 10/07/2023

Keywords:

Hollow-fiber production,

Nonsolvent-induced phase separation,

Dry-jet wet spinning,

Taguchi,

Process control.

***Corresponding author:**

rugbania@cput.ac.za

Abstract

This research proposes a general formula for implementing in the control system of a dry-jet wet spinning machine to achieve a specific diameter size for Polysulfone hollow fibers. By employing Taguchi method, the effect of the operation parameters on the fiber geometry is investigated. The findings emphasize the significance of various fabrication parameters in determining the inner diameter (ID) and outer diameter (OD) of the hollow fibers. To mathematically predict the ID and OD, a first-order equation is developed using the least squares method. The accuracy of the proposed equation is validated through a series of experiments, where the ID and OD of the produced hollow fibers are determined using cross-sectional images by a scanning electron microscope. The results demonstrate a strong agreement between the proposed equation and the experimental data, with a maximum error of less than 7%. This research offers a valuable tool for optimizing hollow-fiber spinning plants and holds promise for improving their overall performance.

1. Introduction

The spinning of hollow fibers involves a complex process, necessitating a comprehensive comprehension of the various manufacturing factors that impact the geometry and characteristics of the fibers. These parameters include the diameter, wall thickness, strength, and porosity of hollow fibers [1-6]. Producing hollow fibers with the required characteristics should involve strict control during the fabrication process over these parameters.

In this research, the investigation is focused on the possibility of controlling inside and outside diameter (ID and OD) sizes during the production of hollow fibers with an OD of less than 1.2 mm. The results are expected to contribute to development of a reliable and reproducible fabrication process for producing hollow fibers with a desired diameter size [7]. The science of manufacturing hollow-fibers involves a good understanding of the various formulation variables and their reciprocal actions. Proper control and manipulation of these

variables can result in producing hollow fibers with the desired properties [8-13]. The studied hollow fibers are used for water ultrafiltration membranes. The main focus of this research is to identify and to regulate the factors that impact the geometry of asymmetric polysulfone (PS) hollow fibers produced through the dry-wet jet spinning process. To achieve this, some experiments are planned based on the Taguchi method. The objective of the experiments is to analyze the significance of different spinning parameters and to evaluate the effect of each parameter in relation to the resulting geometry of the hollow-fiber product.

2. Spinning parameters

By varying the material, concentration, and the manufacturing conditions, it is possible to produce hollow fibers with wide variety of sizes, morphological structures, and mechanical properties [14]. To obtain desired characteristics, it is important to strictly optimize all the interrelated factors and variables during the spinning process [1, 6, 15]. The factors investigated in this research and their limitations are discussed briefly in the following section.

2.1. Dope extrusion rate (DER)

Refers to the solution flow rate, DER is a significant factor influencing the performance of the hollow fibers used in water filtration. Idris *et al.* [16] observed the performance of hollow-fiber membranes produced at DER varying between 2.5 and 4.0 mL/min. Properties of the dope solution affects its spinnability and hence its performance. Solution spinnability refers to its ability to be transformed into a continuous filament without interruptions or irregularities [17]. Through a comparison of membranes produced at various DER within each trial while maintaining the bore fluid, it was noted that the permeability of the membranes varied with changes in the DER. Alsalhy *et al.* [18] concluded that an increase in DER leads to an increase in the porosity of the Polyethersulfone hollow-fiber membrane.

2.2. Bore flow rate (BF)

BF refers to the inner spinneret solution flow rate. High BF applies pressure on the inner fiber surface which, expand the fiber circumference of the inner surface, leading to thin fiber walls [5]. An increase in BF can also contribute to an increase in gas permeance and selectivity due to the resulting thinner fiber wall, which can enhance gas permeance and selectivity properties [19]. Çulfaz *et al.* [20] reported that when the BF is high, the microstructure is affected. This is due to the buckling of the inner surface as a result of shrinkage of the outer fiber surface. Alsalhy *et al.* [18] compared the effect of using different bore types at different flow rates on the properties of PES hollow-fiber membranes. The results proved that BF rate does not have significant effect on the pore size of the hollow fiber.

2.3. Air gap (AG) condition

The AG length is the distance between the spinneret and the coagulation bath. Its length and conditions play a crucial role in determining the membrane geometry and morphology [21]. Wang *et al.* [22] claimed that the effect of decreasing AG from 15 to 5 cm results is thinner separation layer and an increased pure water permeability. Chung and Hu [23] found that increasing AG distance lowers the permeance of the Polyethersulfone hollow-fiber membranes. According to Miao *et al.* [24], the use of different AG of 14.4 cm and 16.1 cm during the spinning process results in hollow fibers with a distinct morphological structure near the outer skin. In a study by conducted Chau *et al.* [25], it was found that the optimal PS hollow-fibers could be achieved at AG = 7 cm. Additionally, Khayet [26] investigated a range of AG lengths from 1 cm to 80 cm on PVDF hollow fiber. The findings indicated that as the AG length increased, there was a decrease in permeability and an increase in rejection rate. Furthermore, the membranes exhibited a denser sponge-type structure at higher air gap lengths. In general, increasing Ag allows for a enough duration for the fibers before entering the coagulation bath, facilitating proper skin formation. However, it is important to avoid

excessively long exposure times, as they can negatively impact the performance of the membranes. Sharpe *et al.* [27] demonstrated that by increasing the residence time in the air gap, selectivity increased and flux decreased as the skin matured and formed effectively. On the other hand, incomplete skin formation is more likely to occur at lower residence times.
It is worth noting that the spinning velocity is a dependent parameter because gravity within AG causes stretching of the extruded filaments [27]. This influence becomes more significant when AG is large and the dope solution viscosity is low. In general, as AG increases, ID and OD of the fiber decrease due to the gravitational force effect [28, 29].

2.4. Take-up speed (TUP)

Precise control over fiber properties like pore size and asymmetry necessitates slow spinning speeds. For example, it is possible to spin polypropylene hollow fibers at TUP as low as 0.76 m/min [30]. Kim *et al.* [31] achieved successful wet-spinning at speeds of 10 – 35 m/min. In the case of polyester, spinning at approximately 3000 m/min and subsequent post-drawing with a 2:1 draw ratio reduces diameter while maintaining strength comparable to fibers spun at 6000 m/min [32]. Higher TUP produces fibers with better chain orientation and packing, which increases selectivity but reduces permeability. The elongation stresses due to higher TUP during spinning alters the fiber morphology. Generally, when TUP increases from 19 to 33 m/min, the gas permeance decreases [19]. The permeation results reported by Mubashir *et al.* [33] revealed that at the TUP ranging from free fall to 12.2 m/min, the CO_2 permeances were dramatically dropped, and selectivities were significantly enhanced by increasing TUP.

2.5. Coagulation bath temperature

The temperature of the coagulation bath, in combination with AG length, has a notable effect on the membrane production and performance [34]. Yeow *et al.* [35] investigated the impacts of coagulation bath temperature on the permeation properties of the produced membrane. The results indicated that higher coagulation temperatures have advantages in hollow fiber production, resulting in increased permeation rates. Furthermore, membranes produced at higher coagulation temperatures displayed a larger pore radius compared to the ones prepared at lower temperatures. Wang *et al.* [36] produced polyvinylidene fluoride membranes using coagulation bath temperatures of 15, 25, and 60 °C. It was reported that more shrinkage and denser fiber surface is obtained at low temperatures. Furthermore, a porous surface can be achieved if the solvent is added to the coagulation bath [36].

3. Experimental setup

3.1. Experimental materials

Polysulfone Udel-3500 in powder form was selected as the polymer material. The solvent was N-methyl-2-pyrrolidone (NMP). The dope solution consisted of polymer/solvent PS: NMP concentration of 18:82. Distilled water was used as the bore fluid.

3.2. Spinning procedure

The hollow-fibers were produced using the nonsolvent-induced phase separation (NIPS) process. [37]. The schematic of the spinning apparatus is illustrated in Fig. 1. The process involved feeding a polymer / solvent solution into a heat-controlled tank. After preparing the machine and degassing the dope solution, the spinning process can be initiated. A pressurized nitrogen gas at 2 bar was used to pump both the bore and dope tanks. The valve of the dope tank was opened, allowing the dope solution to drain into the extrusion pump. Simultaneously, the valve of the bore tank was opened, enabling the bore fluid to flow in the center hole of the spinneret. The dope solution was then pushed through the filter by the metric pump and delivered to the outer ring of the spinneret at the desired DER. As a result, hollow-fiber filaments started to extrude, passed through the air gap, and entered the preheated coagulation bath.
The take-up drum was initiated, and its angular velocity was adjusted accordingly.

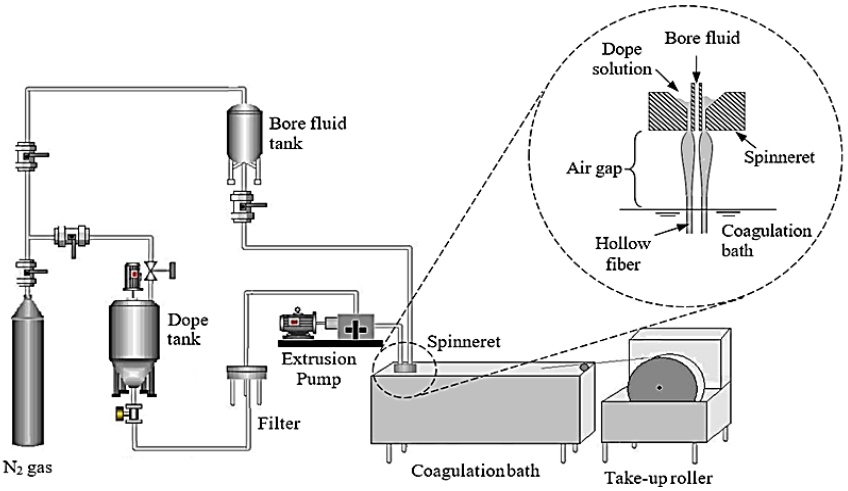

Fig. 1. NIPS dry-jet wet spinning apparatus, with closer look on the spinneret area.

The hollow fiber was kept wet throughout the spinning process. Upon completion, the fibers were removed from the drum, resulting in a bundle length approximately equal to the circumference of the winder (1.22 m).

4. Design of experiments

The Taguchi method was employed in the study to analyze and determine the parameters that influence the geometry and their respective degree of significance. The approach involves identifying the quality characteristics associated with the results using Signal-to-Noise (S/N) ratio [38]. The "smaller-the-better" S/N was chosen to investigate both ID and OD sizes, as the aim was to reduce diameter sizes. Additionally, statistical analysis of variance (ANOVA) was applied to assess the significance level of each parameter on both ID and OD of the hollow fiber.

4.1. Planning of experiments

Based on an initial investigation of eight variables at three levels, five variables were identified as having a significant effect on diameter size and were selected for further study. Linear behavior was considered for these variables within the range of levels investigated. Each run was repeated several times, and the average result was reported to obtain the ID and OD. For a fixed spinneret size, five controllable factors were identified, namely solution temperature (ST), air gap length (AG), bore flow rate (BF), dope extrusion rate (DER), and take-up speed (TUP). Table 1 shows the factors and levels used in each set. In a previous study [5], the coagulant and bore solution temperatures showed no significant effect, so they were eliminated. The L8 OA is sufficient for the examination of seven factors of two-level each, while columns A and G are kept empty.
Table 2 displays the L8 array used in the experiment, along with the assignments to the columns. The numbers within the table represent the levels of the factors. Columns A and G in the table are not assigned to any factors.

Table 1. Factors and their levels.

Factors	levels	
	1	2
A: not used		
ST: (°C)	35	55
AG: (mm)	5	14
BF: (mL/min)	3.5	5.25
DER: (mL/min)	7	11
TUP: (m/min)	1x	1.5x
G: not used		

Table 2. Taguchi's L8 orthogonal array.

Exp no.	Factors						
	A	ST	AG	BF	DER	TUP	G
1	1	1	1	1	1	1	1
2	1	1	1	2	2	2	2
3	1	2	2	1	1	2	2
4	1	2	2	2	2	1	1
5	2	1	2	1	2	1	2
6	2	1	2	2	1	2	1
7	2	2	1	1	2	2	1
8	2	2	1	2	1	1	2

4.2. Confirmation experiments

This stage was aimed to validate the suggested equations for predicting the ID / OD sizes, ensuring their accuracy and reliability in achieving the desired dimensions. The proposed equations were implemented in the control system of the machine, where the factors were controlled and adjusted to produce the required diameter sizes. The confirmation tests were conducted to investigate the individual effect of each factor by performing experiments where one factor was varied while keeping all other factors at constant values. This approach allowed for a more detailed examination of the impact of each factor on the outcomes of interest. The control system can control the input factor values and predict diameter sizes. These predicted results were compared with actual diameter size of the product. Table 3 shows the test values used in each confirmation test.

5. Results and discussion

Scanning electronic microscopy (SEM) was used to image cross-sectional view of 5 samples from each experiment, and the average ID and OD were recorded. Since the smaller fiber diameter is desired. The smaller-the-better target of the S/N ratio (η) is mathematically defined as:

$$\eta_i = -10 \times \log (SQ) \quad (1)$$

where SQ is the average squared deviation.
ANOVA analysis involves determining the percentage contribution (Ω) of each factor and its variance ratio. Ω for a specific factor can be calculated as follows:

$$\Omega = \frac{SQ_f}{SQ_{total}} \quad (2)$$

where SQ_f is the factor's squared deviations, and SQ_{total} is the total of squared deviations.

5.1. Analysis of experimental data

Based on the L8 array, 8 experiments were conducted. The mean S/N ratios of each level for the five factors are shown in Figs. 2 and 3, respectively. The figures indicate that the highest S/N response for each level corresponds to the smallest diameter, as the logarithmic function in Eq. (2) is inversely related to the diameter.

It is observed that TUP has the most significant influence on both the ID and OD, with the minimum diameter achieved at the highest TUP level. It can also be observed that ST exhibits the least impact compared to the other factors, suggesting its influence can be disregarded.
Additionally, AG factor demonstrates a notable contribution in both figures, although its influence is slightly lower compared to TUP.
The BF factor demonstrates a significant effect on the ID of the hollow-fibers but does not have a notable impact on the OD. Increasing the BF leads to increased pressure applied on the inner wall of the hollow fiber, causing it to expand. As a result, the wall thickness is reduced. To compensate for this axial elongation, the TUP needs to be increased.
On the other hand, the DER factor influences the OD but does not significantly influence the ID. An increased amount of dope solution extrusion directly increases the OD and, consequently, increases the wall thickness. However, ID is not significantly affected due to the pressure of BF applied on the inside surfaces. Furthermore, an ANOVA was conducted separately for each response to identify the variables that have statistical significance.

5.2. ANOVA analysis

The ANOVA results of ID presented in Table 4 shows that factors ST and DER do not exhibit significant contributions to the ID. As a result, they were pooled into the error term. On the other hand, TUP, BF and AG were found to be the most significant with confidence levels exceeding 95%. TUP has the highest contribution, accounting for 64% of the total variance in the ID. BF and AG shared a lower relative effect, contributing to approximately 36% of the variance combined. According to the OD results presented in Table 5, factors ST and BF do not have a significant contribution to the OD of the hollow fibers.

Table 3. Values for each factor used for the confirmation experiments.

Factor	Levels			
TUP	1x*	1.5x	2x	2.5x
AG (mm)	5	8*	15	20
DER (mL/min)	4.8	6*	7.8	9.3
BF (mL/min)	2	3	4*	5

* Fixed values utilized when testing other factors.

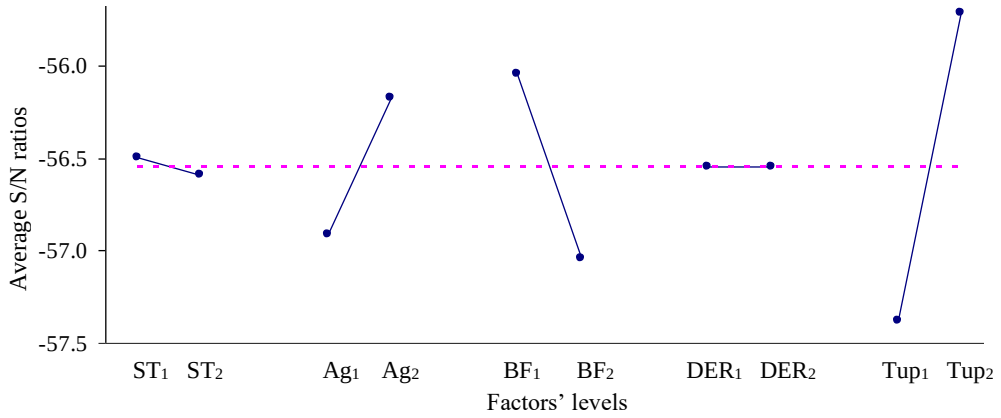

Fig. 2. Factor effects on ID.

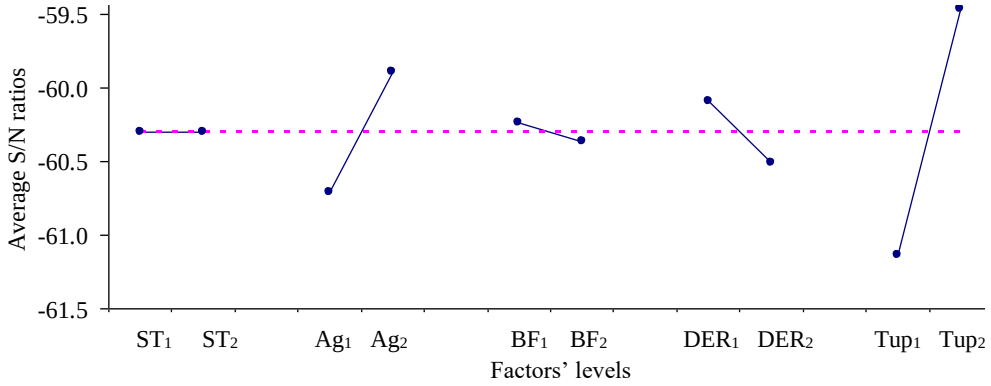

Fig. 3. Factor effects on OD.

As a result, they were merged into the error. TUP has the highest contribution, which accounts for 76% of the total variance. AG has a relatively lower but still significant effect, contributing to 19% of the variance. DER has the least impact on the OD, with only 5% contribution.

The variance ratio (P) in Tables 4 and 5 represents the ratio of the mean square due to a specific factor to the residual mean square (error). The FDIST function in MS Excel is used to calculate the probability distribution, which helps to determine the degrees of freedom. Factors with a confidence level of 95% or higher are considered statistically significant.

A P value less than 1 indicates that the effect of the factor is less than the error, indication that the factor is insignificant. On the other hand, a P value greater than 4 suggests that the factor is significant. Therefore, the P value can be used to rank the factors in terms of their importance.

Table 4. ANOVA results for ID.

Factor	ID				
	SQ	Ω (%)		P	Conf (%)
A					
B: ST	0.02	0	p	2.71	83.9
C: AG	1.10	13		188.9	99.9
D: BF	1.97	23		337.5	99.9
E: DER	0.00	0	p	0.00	1.5
F: TUP	5.52	64		947.4	99.9
G					

Table 5. ANOVA results for OD.

Factor	OD				
	SQ	Ω (%)		P	Conf (%)
A					
B: ST	0.00	0	p	0.01	5.4
C: AG	1.36	19		175.	99.9
D: BF	0.03	0	p	4.35	90.8
E: DER	0.34	5		44.0	99.8
F: TUP	5.54	76		719.	99.9
G					

5.3. Regression model

The ANOVA analysis results confirmed that ID is dependent on AG, BF, and TUP, while the OD is a function of AG, DER, and TUP. The regression analysis of ID and OD can be represented by the following first-order equations:

$$ID = 872 - 5.5\,AG + 44.8\,BF - 275\,TUP \quad (3)$$

$$OD = 1466 - 10.3\,AG + 13.3\,DER - 394\,TUP \quad (4)$$

Eqs. (3 and 4) can be applied within the following limits of the factors (AG: 5 – 14 mm, BF: 3.5 – 5.25 mL/min, TUP: 1x – 1.5x, DER: 7 – 11 mL/min). Fig. 4 presents a visual comparison between Eqs. (3 and 4) and the actual measured values.

6. Confirmation of results

Confirmation tests were conducted individually on the four most significant factors, namely for TUP, AG, BF, and DER.

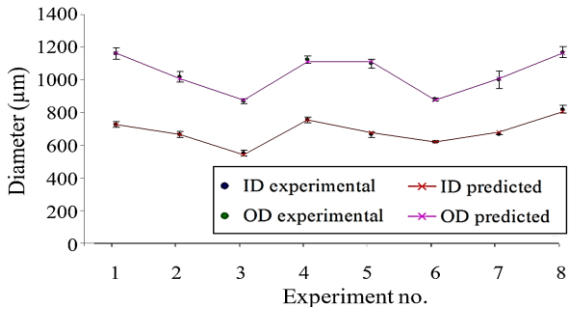

Fig. 4. Comparison of predicted and experimented ID/OD.

By isolating these factors and keeping all other parameters fixed, their specific effects on the geometry of the hollow fibers could be studied in detail. The predicted ID and OD results obtained by Eqs. (3 and 4) were compared with the average diameter sizes. SEM images were used to measure the ID and OD on a cross-sectional view.

6.1. Take-up speed

The only variable parameter here was the TUP. SEM images presented in Fig. 5 demonstrate that increasing TUP beyond twice its minimum value leads to fibers with irregular inner contours, displaying more pronounced deformations. Similar observations were made by Santoso et al. [39], who explored the influence of high-speed spinning on inner skin morphology and proposed potential solutions to address this issue.

The experimentally measured ID and OD values were determined by averaging the measurements of 3 samples. The ID and OD were predicted using Eqs. (3 and 4), respectively.

Fig. 6 illustrates a comparison between the experimental and predicted results, showing good agreement up to a TUP of double the minimum speed, with an error of less than 7.8% within the investigated range.

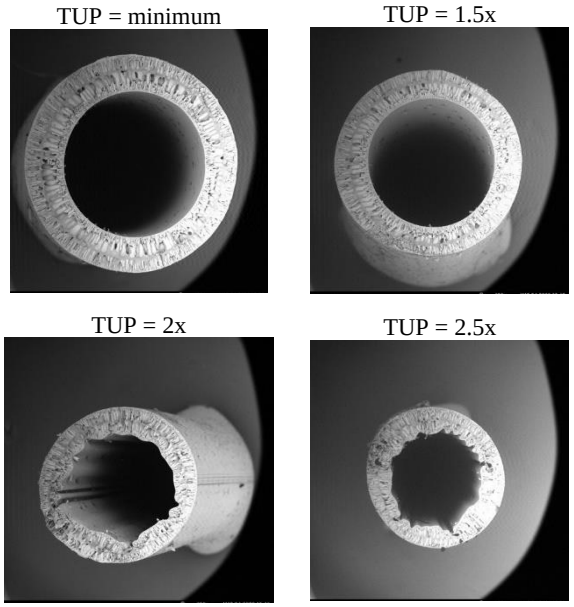

Fig. 5. SEM images of fibre prepared at different TUP (150x magnification).

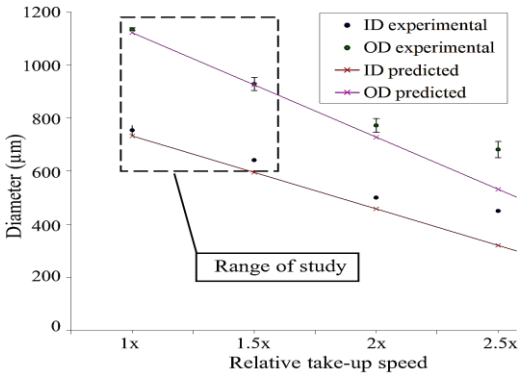

Fig. 6. Experimental measurements and predicted values of ID and OD at various relative TUP.

The results obtained from the model begin to deviate when the TUP exceed double the minimum speed, as depicted in Fig. 6. It is worth noting that higher TUP speeds are not desirable due to their adverse impact on the inner shape of the hollow-fibers, which consequently affects their overall performance.

6.2. Bore flow rate

Fig. 7 displays SEM images of each experiment, illustrating the influence of the BF value on the ID of the hollow fibers. It is evident from the images that changes in BF have a noticeable impact on the ID, while the OD remains relatively unaffected. This indicates that adjusting the BF serves as a means to modify the wall thickness of the fibers [5]. The experimental and predicted values of both ID and OD are presented in Fig. 8. The predicted OD remained stable as BF does not affect OD, as indicated by Eq. (4). The experimental measurements of OD also exhibit minimal deviation. Overall, the predicted values of ID and OD closely align with the experimental results, demonstrating an error of less than 6.8%.

6.3. Air gap length

The SEM images depicted in Fig. 9 demonstrate a slight reduction in both ID and OD as the AG distance increases from 5 mm to 20 mm. This observation aligns with the experimental measurements and predicted values shown in Fig. 10, where increased AG distance leads to a decrease in both ID and OD of the fiber. This effect can be attributed to the gravitational force impact on the fiber during the spinning process [28, 29]. The predicted results from the model for ID and OD and the experimental measurements shown in Fig. 10 show an acceptable match within the range of the study. The maximum error between the model and the experimental measurements was less than 3%.

6.4. Dope extrusion rate

The SEM images presented in Fig. 11 illustrate that increasing the DER influence the OD, while no significant change in the ID is observed. The experimental and predicted diameter results are displayed in Fig. 12.

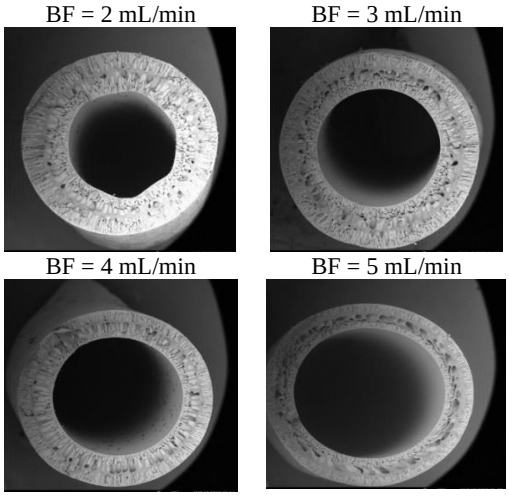

Fig. 7. SEM images of fibre prepared using different BF (150x magnification).

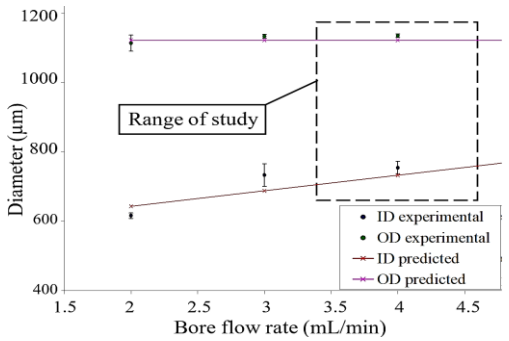

Fig. 8. Experimental measurements and predicted values of ID and OD at various BF.

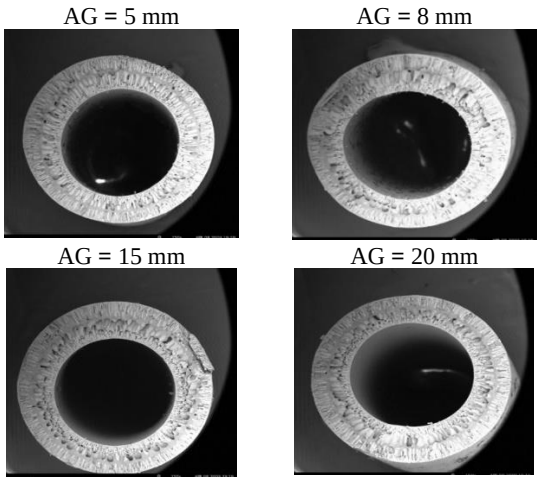

Fig. 9. SEM images of fiber prepared using deferent AG (150x magnification).

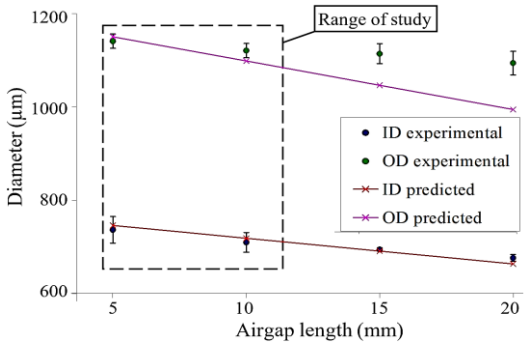

Fig. 10. experimental measurements and predicted values of ID and OD at various AG.

According to the prediction model, Eq. (3), the ID values remain unaffected by changes in the DER. This is attributed to the neglected effect of the DER factor on the ID. As DER increases, the OD of the fiber increases, while the ID remains relatively unchanged.

This is due to the pressure exerted by the bore solution on the inner surface of the hollow fiber [16]. Generally, the experimental measurements of both ID and OD agree with the predicted results with an error of less than 3.7% within the investigated range shown in Fig. 12.

7. Conclusions

The study investigated the influence of various process parameters on the geometry of Polysulfone hollow fibers produced using the dry-jet wet spinning technique. The Taguchi experimental design method was utilized to examine the effect of various spinning parameters. The results of Taguchi's method demonstrated that the TUP, AG length, DER, and BF parameters have significant effects on the ID and OD and hence the wall thickness of the hollow fibers.

In addition, regression models utilizing the significant factors were established to predict ID and OD of the hollow fibers. The equation for predicting ID was determined to be dependent on TUP, AG, and BF, while the equation for predicting OD was dependent on TUP, AG, and DER. To validate the equations, confirmation experiments were conducted, and the diameters of the hollow fibers were measured using SEM.

The results from the model demonstrated strong agreement with the experimental measurements, with an error of less than 7%.

The study presents a promising approach to control the fabrication process of Polysulfone hollow fibers with specific geometries and characteristics using the proposed regression models. The results suggest that the control model could be implemented in the control system of the spinning machine to ensure consistent production of hollow fibers with desired properties. Further studies could focus on optimizing the process parameters for other types of hollow fibers and investigating the effects of other factors on the hollow fiber properties.

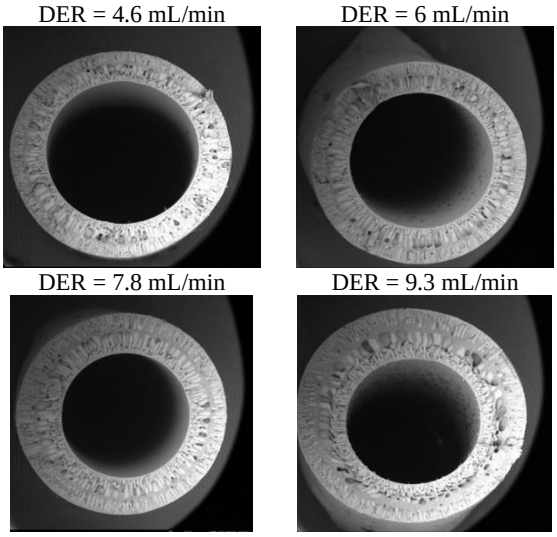

Fig. 11. SEM of fiber prepared using different DER (150x magnification).

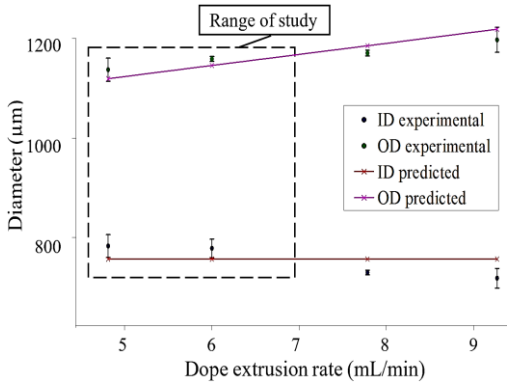

Fig. 12. experimental measurements and predicted values of ID and OD at various DER.

References

[1] H. Yücel and P. Z. Çulfaz-Emecen, "Helical hollow fibers via rope coiling: Effect of spinning conditions on geometry and membrane morphology," *J. Membr. Sci.*, Vol. 559, pp. 54–62, (2018).

[2] K. C. Chong, S. O. Lai, W. J. Lau, H. S. Thiam, A. F. Ismail and A. K. Zulhairun, "Fabrication and characterization of polysulfone membranes coated with polydimethysiloxane for oxygen enrichment," *Aerosol Air Qual Res*, Vol. 17, No. 11, pp. 2735–2742, (2017).

[3] Y. Li, B. Cao and P. Li, "Fabrication of PMDA-ODA hollow fibers with regular cross-section morphologies and study on the formation mechanism," *J. Membr. Sci.*, Vol. 544, pp. 1–11, (2017).

[4] Y. Tang, N. Li, A. Liu, S. Ding, C. Yi and H. Liu, "Effect of spinning conditions on the structure and performance of hydrophobic PVDF hollow fiber membranes for membrane distillation," *Desalination*, Vol. 287, pp. 326–339, (2012).

[5] Q. F. Alsalhy, H. A. Salih, R. H. Melkon, Y. M. Mahdi and N. A. Abdul Karim, "Effect of the preparation conditions on the morphology and performance of poly(imide) hollow fiber membranes," *J. Appl. Polym. Sci.*, Vol. 131, No. 12, (2014).

[6] S. Mansur, M. H. D. Othman, A. F. Ismail, S. H. Sheikh Abdul Kadir, F. Kamal, P. S. Goh, H. Hasbullah, B. C. Ng and M. S. Abdullah, "Investigation on the effect of spinning conditions on the properties of hollow fiber membrane for hemodialysis application," *J. Appl. Polym. Sci.*, Vol. 133, No. 30, (2016).

[7] A. Rugbani, "*Investigating the influence of fabrication parameters on the diameter and mechanical properties of polysulfone ultrafiltration hollow-fibre membranes*," MSc Thesis, University of Stellenbosch, Sout Africa, (2009).

[8] C. F. Wan, T. Yang, G. G. Lipscomb, D. J. Stookey and T. S. Chung, "Design and fabrication of hollow fiber membrane modules," *J. Membr. Sci.*, Vol. 538. pp. 96–107, (2017).

[9] G. Reyes, R. Ajdary, M. R. Yazdani and O. J. Rojas, "Hollow filaments synthesized by dry-jet wet spinning of cellulose nanofibrils: structural properties and thermoregulation with phase-change infills," *ACS Appl Polym Mater*, Vol. 4, No. 4, pp. 2908-2916, (2022).

[10] B. Govardhan, S. S. Chandrasekhar and S. Sridhar, "Purification of surface water using novel hollow fiber membranes prepared from polyetherimide/polyethersulfone blends," *J. Environ. Chem. Eng.*, Vol. 5, No. 1, pp. 1068–1078, (2017).

[11] K. Sankhala, J. Koll, M. Radjabian, U. A. Handge and V. Abetz, "A pathway to fabricate ollow fiber membranes withIsoporous inner surface," *Adv. Mater. Interfaces*, Vol. 4, No. 7, pp. 1600991, (2017).

[12] A. J. Kajekar, B. M. Dodamani, A. M. Isloor, Z. A. Karim, N. B. Cheer, A. F. Ismail and S. J. Shilton, "Preparation and characterization of novel PSf/PVP/PANI-nanofiber nanocomposite hollow fiber ultrafiltration membranes and their possible applications for hazardous dye rejection," *Desalination*, Vol. 365, pp. 117–125, (2015).

[13] M. Naeimirad, A. Zadhoush, R. E. Neisiany, S. Ramakrishna, S. Salimian and A. A. Leal, "Influence of microfluidic flow rates on the propagation of nano/microcracks in liquid core and hollow fibers," *Theor. Appl. Fract. Mech.*, Vol. 96, pp. 83-89, (2018).

[14] M. Naeimirad, A. Zadhoush, R. Esmaeely Neisiany, S. Salimian and R. Kotek, "Melt-spun PLA liquid-filled fibers: physical, morphological, and thermal properties," *J. Text. Inst.*, Vol. 110, No. 1, pp. 89-99, (2019).

[15] H. A. Salih, "*Preparation and characterization of Polyethersulfone hollow fiber ultrafiltration membranes and application in protein separation*,"

MSc. thesis, University of Technology, Iraq, (2012).

[16] A. Idris, A. F. Ismail, M. Y. Noordin and S. J. Shilton, "Optimization of cellulose acetate hollow fiber reverse osmosis membrane production using Taguchi method," *J. Membr. Sci.*, Vol. 205, No. 1–2, pp. 223–237, (2002).

[17] J. Yin, "*Fabrication of grooved hollow fiber membrane for nerve regeneration: process modeling and performance evaluation*," PhD Thesis, Clemson University, (2011).

[18] Q. F. Alsalhy, H. A. Salih, S. Simone, M. Zablouk, E. Drioli and A. Figoli, "Poly(ether sulfone) (PES) hollow-fiber membranes prepared from various spinning parameters," *Desalination*, Vol. 345, pp. 21–35, (2014).

[19] W. F. Yong, T. S. Chung, M. Weber and C. Maletzko, "New polyethersulfone (PESU) hollow fiber membranes for CO2 capture," *J. Membr. Sci.*, Vol. 552, pp. 305–314, (2018).

[20] P. Z. Çulfaz, M. Wessling and R. G. H. Lammertink, "Hollow fiber ultrafiltration membranes with microstructured inner skin," *J. Membr. Sci.*, Vol. 369, No. 1–2, pp. 221–227, (2011).

[21] F. Korminouri, M. Rahbari-Sisakht, T. Matsuura and A. F. Ismail, "Surface modification of polysulfone hollow fiber membrane spun under different air-gap lengths for carbon dioxide absorption in membrane contactor system," *Chem. Eng. J.*, Vol. 264, pp. 453–461, (2015).

[22] D. Wang, K. Li and W. K. Teo, "Preparation and characterization of polyvinylidene fluoride (PVDF) hollow fiber membranes," *J. Membr. Sci.*, Vol. 163, No. 2, pp. 211–220, (1999).

[23] T. Chung and X. Hu, "Effect of air-gap distance on the morphology and thermal properties of polyethersulfone hollow fibers," *J. Appl. Polym. Sci.*, Vol. 66, No. 6, pp. 1067–1077, (1997).

[24] X. Miao, S. Sourirajan, H. Zhang and W. W. Y. Lau, "Production of polyethersulfone hollow fiber ultrafiltration membranes. I. effects of water (internal coagulant) flow rate (WFR) and length of air gap (LAG)," *Sep. Sci. Technol.*, Vol. 31, No. 2, pp. 141–172, (1996).

[25] C. J. Lee, S. S. Wang, G. C. Lin, W. Hu and L. T. Chen, "Pilot production of polysulfone hollow fiber for ultrafiltration using orthogonal array experimentation," *Ind. Eng. Chem. Res.*, Vol. 34, No. 3, pp. 813–819, (1995).

[26] M. Khayet, "The effects of air gap length on the internal and external morphology of hollow fiber membranes," *Chem. Eng. Sci.*, Vol. 58, No. 14, pp. 3091–3104, (2003).

[27] I. D. Sharpe, A. F. Ismail and S. J. Shilton, "A study of extrusion shear and forced convection residence time in the spinning of polysulfone hollow fiber membranes for gas separation," *Sep. Purif. Technol.*, Vol. 17, No. 2, pp. 101–109, (1999).

[28] M. Khayet, M. C. García-Payo, F. A. Qusay and M. A. Zubaidy, "Structural and performance studies of poly(vinyl chloride) hollow fiber membranes prepared at different air gap lengths," *J. Membr. Sci.*, Vol. 330, No. 1–2, pp. 30–39, (2009).

[29] I. M. Wienk, F. H. A. Olde Scholtenhuis, T. van den Boomgaard and C. A. Smolders, "Spinning of hollow fiber ultrafiltration membranes from a polymer blend," *J. Membr. Sci.*, Vol. 106, No. 3, pp. 233–243, (1995).

[30] J. J. Kim, T. S. Jang, Y. D. Kwon, U. Y. Kim and S. S. Kim, "Structural study of microporous polypropylene hollow fiber membranes made by the melt-spinning and cold-stretching method," *J. Membr. Sci.*, Vol. 93, No. 3, pp. 209–215, (1994).

[31] J. -H Kim, Y. -I Park, J. Jegal and K. -H Lee, "The effects of spinning conditions on the structure formation and the dimension of the hollow-fiber membranes and their relationship with the permeability in dry–wet spinning technology," *J. Appl. Polym. Sci.*, Vol. 57, No. 13, pp. 1637–1644, (1995).

[32] A. De Rovere, B. P. Grady and R. L. Shambaugh, "The influence of processing parameters on the properties of melt-spun polypropylene hollow fibers," *J. Appl. Polym. Sci.*, Vol. 83, No. 8, pp. 1759–1772, (2002).

[33] M. Mubashir, Y. F. Yeong, T. L. Chew and K. K. Lau, "Optimization of spinning parameters on the fabrication of NH 2 - MIL-53(Al)/cellulose acetate (CA) hollow fiber mixed matrix membrane for CO 2 separation," *Sep. Purif. Technol.*, Vol. 215, pp. 32–43, (2019).

[34] L. García-Fernández, M. C. García-Payo and M. Khayet, "Mechanism of formation of hollow fiber membranes for membrane distillation: 1. Inner coagulation power effect on morphological characteristics," *J. Membr. Sci.*, Vol. 542, pp. 456–468, (2017).

[35] M. L. Yeow, Y. Liu and K. Li, "Preparation of porous PVDF hollow fibre membrane via a phase inversion method using lithium perchlorate (LiClO 4) as an additive," *J. Membr. Sci.*, Vol. 258, No. 1–2, pp. 16–22, (2005).

[36] X. Wang, L. Zhang, D. Sun, Q. An and H. Chen, "Effect of coagulation bath temperature on formation mechanism of poly(vinylidene fluoride) membrane," *J. Appl. Polym. Sci.*, Vol. 110, No. 3, pp. 1656–1663, (2008).

[37] F. Tasselli, "Non-solvent induced phase separation process (NIPS) for membrane preparation," *in Encyclopedia of Membranes*, Springer, Berlin, Heidelberg, (2014).

[38] R. K. Roy, *A primer on the Taguchi method*, 1st ed., Michigan: Society of Manufacturing Engineers, (1990).

[39] Y. E. Santoso, T. S. Chung, K. Y. Wang and M. Weber, "The investigation of irregular inner skin morphology of hollow fiber membranes at high-speed spinning and the solutions to overcome it," *J. Membr. Sci.*, Vol. 282, No. 1–2, pp. 383–392, (2006).

How to cite this paper:

A. Rugbani, "Predictive model for diameter control of polysulfone hollow fibers produced by dry-jet wet spinning,", *J. Comput. Appl. Res. Mech. Eng.*, Vol. 13, No. 1, pp. 27-38, (2023).

DOI: 10.22061/JCARME.2023.8916.2202

URL: https://jcarme.sru.ac.ir/?_action=showPDF&article=1903